

Synthesis and physiochemical investigations of imidazolium 4-hydroxybenzoate (I4HB) for nonlinear optical applications

E Shobhana*^a, B Babu^b, R Kannan^c & R Thirumurugan^d

^aDepartment of Physics, Kumaraguru College of Technology, Coimbatore 641 049, Tamil Nadu, India

^bDepartment of Physics, KPR Institute of Engineering and Technology, Coimbatore 641 407, Tamil Nadu, India

^cDepartment of Physics, Basic Engineering, Sakthi Polytechnic College, Erode 638 315, Tamil Nadu, India

^dDepartment of Physics, Easwari Engineering College, Chennai 600 089, Tamil Nadu, India

E-mail: shobhana.r.sci@kct.ac.in, shobhyphysics@gmail.com

Received 16 February 2024; accepted (revised) 29 May 2024

The slow evaporation approach has been used to produce and develop imidazolium 4-hydroxybenzoate (I4HB), a novel organic proton-transfer chemical substance. Through single-crystal X-ray diffraction, detailed study shows a monoclinic crystal structure with the centrosymmetric space group $P2_1/n$. Vibrational modes have been investigated using FT-IR and FT-Raman spectroscopy. The chemical structure of the molecule has been thoroughly validated using ^1H and ^{13}C NMR analysis. UV-Vis-NIR absorption spectra have been used to investigate electronic transitions. Thermal parameters such as a melting point of 215°C and breakdown phases have been investigated using TG-DTA analysis. Third-order nonlinearity has also been confirmed using Z-scan analysis.

Keywords: X-ray diffraction, NMR spectral analysis, TG-DTA analysis, Z-scan

Currently, a lot of attention has been devoted for achieving “multi-component molecular crystals” in the frontier area of pharmaceutical, material science and other industrial applications¹. Crystals of multicomponent molecules represent molecular solids composed of at least two distinct chemical entities, encompassing neutrals, salts, hydrates, solvates, clathrates, among others. The organization of molecules in these crystals is primarily dictated by hydrogen bonding interactions. Formations of molecular crystals have been extensively offering some admirable features of modifying important physicochemical perspectives to aim desired nonlinear optical applications². Accordingly, in the pharmaceutical industry this strategy has been widely utilized to enhance physicochemical characteristics and therapeutic efficiencies over parent drugs³. Also, the formation of molecular crystal is valuable in lessening side effects in the parent drugs. In this context, in particular, the stability and bioavailability of active pharmaceutical ingredients can be improved by formulating them as hydrates or salts. In this scenario, intermolecular interactions between hydrogen bonds as well as van der Waals forces are crucial in producing multicomponent solids with the necessary

components⁴. In frontier area of materials science, formation of multicomponent crystals is an emerging technique broadly discussed in achieving organic Nonlinear optical (NLO) crystals that exhibits enormous applications such as photonics and optoelectronics⁵⁻⁸. In recent times, intriguing multi-component crystals have been created through the utilization of imidazole, a widely recognized organic base molecule known for its propensity to readily form proton transfer complexes. For example, imidazole-imidazolium picrate monohydrate, imidazolium dipicolinate and imidazolium L-tartrate⁹⁻¹¹. In similar way, 4-hydroxybenzoic acid is a familiar organic compound widely employed in forming pharmaceutical multicomponent crystals¹²⁻¹⁹. Based on the above facts, imidazole has been planned to complex with 4-nitrobenzoic acid to form multicomponent crystals and study its essential properties for biological recognition. As reported²⁰, in prior studies, researchers successfully synthesized the crystalline structure of 1*H*-Imidazol-3-ium 4-hydroxybenzoate. The synthesis process resulted in a well-defined monoclinic crystal arrangement, which was characterized using the $P2_1/c$ space group system. This crystallographic configuration provides essential insights into the compound's atomic

arrangement, aiding in a comprehensive understanding of its properties and behavior. The unit cell dimensions were as follows: $a = 9.616(1) \text{ \AA}$, $b = 10.587(2) \text{ \AA}$, $c = 11.075(5) \text{ \AA}$, $\beta = 118.93(2)^\circ$, and the volume was 986.8 \AA^3 . However, in this current investigation, the crystal structure of I4HB displays a monoclinic crystal system with the P21/n space group and new unit cell parameters: $a = 9.587(3) \text{ \AA}$, $b = 10.519(2) \text{ \AA}$, $c = 10.543(5) \text{ \AA}$, $\beta = 113.72(3)^\circ$, with a volume of 973.39 \AA^3 . Notably, this arrangement exhibits a different molecular packing compared to the previous one. The molecular crystal of I4HB obtained in this study was subjected to several experimental characterizations, including single crystal X-ray diffraction, NMR, FTIR, FT-Raman, UV-Vis spectral analysis, and thermal studies using TG-DTA.

Experimental Section

Synthesis of the I4HQ compound

All chemicals were procured in AR grade from Merck Chemical Co. with a purity $\geq 98.0\%$, and they were utilized in the synthesis process as received. An equal proportion of imidazole (0.34 g, 0.5 mol) and 4-hydroxybenzoic acid (0.69 g, 0.5 mol) was dissolved in 20 mL of ethanol as the solvent. The solution was continuously stirred and subjected to 2 h of sustained stirring on a hot plate. This process was employed to synthesize the chemical compound known as imidazolium 4-hydroxybenzoate. The resulting mixture was then filtered, and the filtered solution was placed in a clean petri dish covered with perforated transparent polythene paper to facilitate controlled ethanol solvent evaporation. Small crystalline particles collected from the solution after a week of evaporation, and their quality was improved through successive recrystallization steps using ethanol as the solvent. After a week, an optically transparent I4HB crystal measuring $9 \times 9 \times 1.3 \text{ mm}^3$ was obtained. A colourless, block-shaped single crystal of I4HB with dimensions of $0.32 \times 0.30 \times 0.20 \text{ mm}^3$ was chosen for X-ray diffraction analysis after optical quality assessment. The chemical scheme and a photograph of the as-grown single crystal of I4HB are depicted in Fig. 1(a-b).

Characterization Techniques

A detailed and exhaustive structural analysis was carried out using a BRUKER ENRAF NONIUS CAD4 diffraction spectrometer, where X-ray diffraction intensity data was meticulously gathered and studied. This sophisticated analysis provided

valuable insights into the crystal's atomic arrangement and helped in understanding its structural properties in depth. The analysis employed the ω -2 θ scan method, maintaining the temperature at RT throughout the experiment. The system employed graphite monochromated Mo K X-rays having an effective wavelength of 0.71073 \AA . The direct method techniques inside the SHELXS-97 software²¹ were used to solve the crystal structure of I4HB, and an anisotropic least-square refinement approach was used to all non-hydrogen atoms using the SHELXL-97 program²¹. Hydrogen atoms were found and permitted to freely ride on non-hydrogen atoms. The molecular structure and molecular crystal packing diagram of I4HB were constructed in three dimensions using the Ortep-3 (Ref. 22) and Mercury-3.8 software²³.

The ^1H and ^{13}C NMR spectra of the I4HB compound were recorded using a Bruker 500 MHz spectrometer with DMSO- d_6 as the solvent. The FTIR spectrum for I4HB was obtained using the KBr pellet method on a Shimadzu IR Affinity-1S FTIR spectrophotometer in the spectral range of $4000\text{--}400 \text{ cm}^{-1}$. A Shimadzu UV-2400 PC series spectrophotometer was also used to record the absorption spectra for I4HB. Perkin-Elmer Simultaneous Thermal Analyzer (STA) 8000 equipment were used to perform simultaneous TG-DTA measurements at a heating rate of $20^\circ\text{C}/\text{min}$.

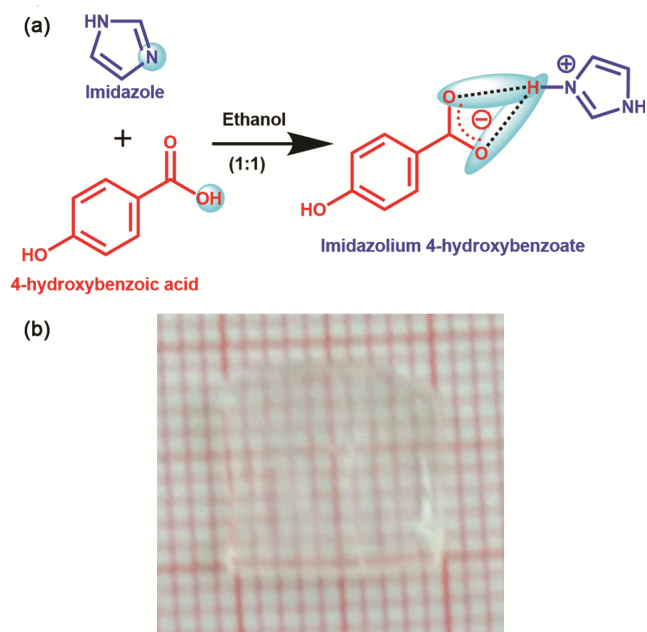


Fig. 1 — (a) The chemical scheme of I4HB compound; (b) Photograph of I4HB single crystal

Results and Discussion

Analysis of Crystal Structure

The crystal structure of I4HB ($C_{10}H_{10}N_2O_3$) exhibits monoclinic system within the $P2_1/n$ space group, with one molecule of protonated imidazole ($C_3H_5N_2^+$) in its cationic form and one deprotonated 4-hydroxybenzoic acid ($C_7H_5O_3^-$) in its anionic form contained within the asymmetric unit. The transfer of a proton from 4-hydroxybenzoic acid to the imidazole molecule is illustrated in Fig. 1a (chemical scheme). Crystallographic and refinement details were presented in Table 1. The selected intermolecular hydrogen bonding interactions of I4HB are listed in Table 2. The protonation at the N2 atom of imidazole, as depicted in Fig. 2 (Ortep diagram), is confirmed by the increase in the C8-N2-C10 bond angle ($109.6(5)^\circ$) compared to the C-N-C bond angle (106.09°) of the neutral molecule. Both the imidazolium cation and 4-hydroxybenzoate anion adopt planar configurations, with Root Mean Square Deviations (RMSD) of $0.003(1) \text{ \AA}$ and $0.06(2) \text{ \AA}$, respectively. However, they are oriented parallel to each other with a dihedral angle deviation of 4.54° between their planes. The molecular geometric characteristics of the imidazolium cation and the 4-hydroxybenzoate anion closely align with those reported in prior studies^{24,25}.

In the crystal structure, the carboxylate (COO^-) and hydroxyl (OH) functional groups within the 4-hydroxybenzoate anion play a pivotal role in the formation of strong intermolecular hydrogen bonds. Specifically, the carboxylate group (COO^- , O2-C3-

O1) attached to the anion exhibits a dihedral angle deviation of 4.19° due to the formation of intermolecular hydrogen bonds (N1-H6 \cdots O1; $d/\text{\AA}$, $\theta/^\circ$; 2.673(1), 173.9 (2); N1-H6 \cdots O2; $d/\text{\AA}$, $\theta/^\circ$; 3.054 (1), 124.58 (2)). These interactions involve the protonated N1 atom in the imidazolium cation and the carboxylate oxygen atoms (O1 and O2) in the 4-hydroxybenzoate anion, leading to the creation of a distinctive of $R_1^2(5)$ ring motif²⁶.

Furthermore, the C1-H1 \cdots O1 and C8-H7 \cdots O2 bond angles exhibit torsional characteristics, as evidenced by their bond angle values exceeding 90° . Within the crystal packing, intermolecular hydrogen bonds (N1-H6 \cdots O1, N1-H6 \cdots O2, O3-H3 \cdots O2 and N2-H8 \cdots O2) form a three-dimensional network, as depicted in Fig. 2c along the c-axis. Consequently, it can be concluded that the stability of the I4HB crystal structure primarily arises from significant contributions made by N-H \cdots O, O-H \cdots O and C-H \cdots O intermolecular contacts.

NMR Spectral Analysis

The crystallized compound was characterization via 1H and ^{13}C NMR spectroscopy. In the 1H NMR spectrum Fig. 3a, all peaks were observed within the δ 6.5 – 8.0 ppm range, indicating the presence of aromatic protons in the compound. There are a total of 10 protons in this compound. The 1H NMR spectrum shows 7 protons, as the protons associated with imidazole NH, imidazolium NH, and phenolic hydroxyl groups are labile and may not appear in the spectrum. The presence of a singlet at δ 7.09 for two

Table 1 — Crystal data and structure refinement details of I4HB

Empirical formula	$C_{10}H_{10}N_2O_3$
Formula weight	206.2
Temperature	293(2) K
Wavelength	0.71073 \AA
Crystal system	Monoclinic
Space group	$P2_1/n$
Unit cell dimensions	a = 9.587 (3) \AA $\alpha = 90^\circ$ b = 10.519 (2) \AA $\beta = 113.72 (3)^\circ$ c = 10.543 (5) \AA $\gamma = 90^\circ$
Volume	973.4 (6) \AA ³
Z	4
Density (calculated)	1.407 Mg/m ³
Absorption coefficient	0.106 mm ⁻¹
F(000)	432
θ range for data collection	2.43 to 17.97 $^\circ$
Index ranges	0 < h < 8, -1 < k < 9, -9 < l < 8
Reflections collected	841
Independent reflections	667 (R(int) = 0.0584)
Completeness to $\theta = 25.0^\circ$	100.00%
Absorption correction	None
Refinement method	Full-matrix least-squares on F ²
Data / restraints / parameters	667 / 0 / 176
Goodness-of-fit on F2	1.141
Final R indices (I > 2 σ (I))	R1 = 0.0599, wR2 = 0.1619
R indices (all data)	R1 = 0.0620, wR2 = 0.1669
Largest diff. peak and hole	0.308 and -0.236 e. \AA ⁻³

Table 2 — Selected intermolecular hydrogen bonds of I4HB (\AA and $^\circ$)

D-H...A	d(D-H)	d(H...A)	d(D...A)	<(DHA)
C(1)–H(1) \cdots O(1)#0	0.94(5)	2.52(4)	2.83(1)	99.05(3)
C(4)–H(5) \cdots O(2)#0	0.93(5)	2.56(6)	2.81(1)	95.69(3)
C(5)–H(4) \cdots O(2)#1	0.83(4)	2.99(3)	3.52(1)	124.32(2)
C(8)–H(7) \cdots O(2)#2	0.95(5)	2.63(4)	3.12(5)	112.26(3)
C(8)–H(7) \cdots O(1)#3	0.95(5)	2.45(4)	3.04(6)	119.59(3)
C(10)–H(9) \cdots O(3)#4	0.87(4)	2.58(3)	3.26(7)	135.37(3)
O(3)–H(3) \cdots O(3)#1	1.11(8)	1.51(4)	2.61(4)	169.55(6)
N(1)–H(6) \cdots O(1)#2	0.89(4)	1.79(4)	2.67(5)	173.90(5)
N(1)–H(6) \cdots O(2)#2	0.89(4)	2.46(5)	3.05(1)	124.58(4)
N(2)–H(8) \cdots O(1)#3	0.83(4)	2.77(5)	3.14(7)	108.68(4)
N(2)–H(8) \cdots O(2)#5	0.83(4)	1.95(4)	2.75(5)	160.99(4)

To construct equivalent atoms, symmetry modifications are utilized (#0) x,y,z

(#1) -x+1/2,+y+1/2,-z+1/2

(#2) -x,-y-1,-z+1

(#3) -x+1/2,+y+1/2,-z+1/2+1

(#4) -x+1,-y,-z+1

(#5) x+1/2,-y-1/2,+z+1/2

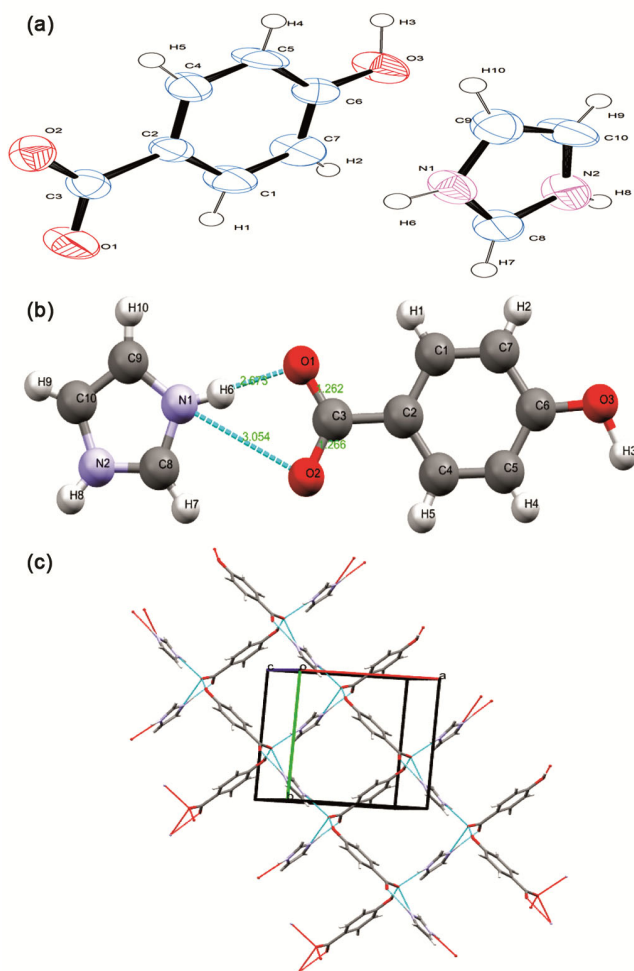


Fig. 2 — (a) The molecular arrangement of I4HB is presented, including atom numbering and the depiction of non-hydrogen atoms with thermal displacement ellipsoids set at a 50% probability level; (b) The protonated N1 atom in the cation and the carboxylate oxygen atoms (O1 and O2) in the anion come together to create a $R_1^2(5)$ ring motif through a pair of intermolecular hydrogen bonds, specifically N1–H6···O1 and N1–H6···O2; (c) The three-dimensional network of I4HB, observed when viewing along the *c*-axis, is created through intermolecular hydrogen bonds (N1–H6···O1, N1–H6···O2, O3–H3···O2 and N2–H8···O2) highlighted as pink dotted lines.

protons and a singlet at δ 7.74 for one proton can be attributed to the imidazolium ring. Furthermore, the occurrence of two sets of doublets at δ 7.85 and 6.88 suggests the presence of the *p*-hydroxybenzoate unit. The fact that these protons exhibit the same coupling constants indicates that they are coupling partners.

Similarly, the ^{13}C NMR also proves the compound formation, which reveals the presence of 7 distinct carbon sets in the compound. As depicted in Fig. 3b, the ^{13}C NMR spectrum clearly displays 6 carbon sets (with the possibility of one quaternary carbon not

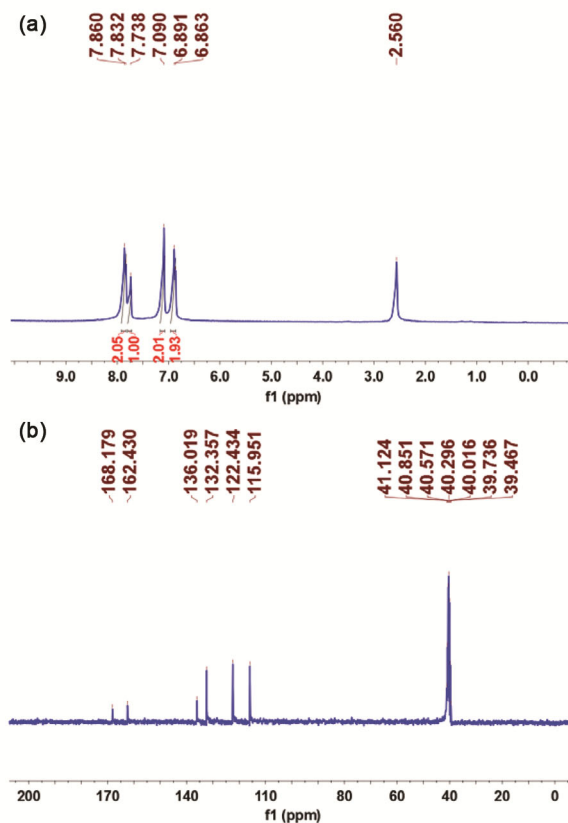


Fig. 3 — (a) ^1H NMR (300 MHz, $\text{DMSO-}d_6$) spectrum; (b) ^{13}C NMR (75 MHz, $\text{DMSO-}d_6$) spectrum

being visible). Notably, the appearance of a peak at δ 168.18 signifies the presence of a carboxylate unit within the *p*-hydroxyphenyl group. Additionally, peaks at approximately δ 115.95 and 132.35 (representing two sets of carbon signals) are attributed to the *ortho* and *meta*-carbons of the *p*-hydroxybenzoate unit. Another peak at δ 123.42 corresponds to the imidazolium C3 and C4 carbons. The quaternary carbon attached to a hydroxyl group is observed at δ 162.43, and a peak at δ 136.01 corresponds to the imidazolium C2 carbon.

Vibrational analysis using FTIR and FT-Raman spectroscopy

FTIR and FT-Raman spectroscopic analyses were performed on the I4HB crystal, and the resulting spectra are depicted in Fig. 4a and Fig. 4b, respectively. The wavenumbers and their corresponding vibrational assignments for the functional groups present in I4HB are detailed in Table 3.

The spectral peaks corresponding to the vibrations of functional groups within both the imidazolium cation and the 4-hydroxybenzoate anion were

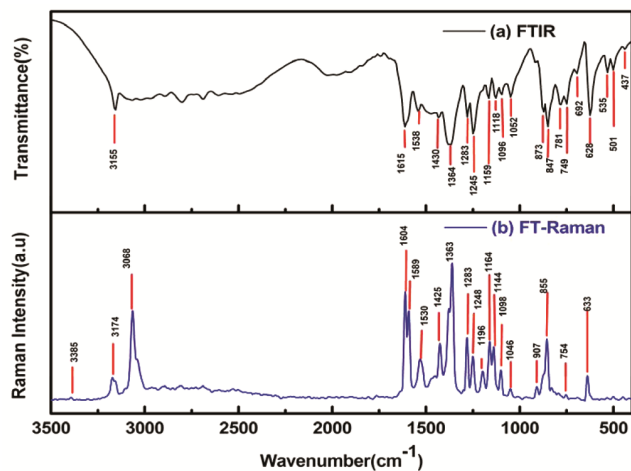


Fig. 4 — (a-b) FTIR and FT-Raman spectra of I4HB

Table 3 — FTIR frequencies along with their vibrational assignments for the I4HB compound

FTIR (cm ⁻¹)	FT-Raman (cm ⁻¹)	Mode of Vibrations
3385(w)		ν N-H \cdots O
3155(w)	3174(w)	ν N-H \cdots O & O-H \cdots O
3068(s)		ν C-H
2034(w)		ν N-H \cdots O
1615(s)	1604(s)	ν_{as} COO ⁻
1538(w)	1530(m)	ν C-C ring
1430(w)	1425(m)	ν_s COO ⁻
1364(s)	1363(s)	ν C-N
1283(w)	1283(s)	ν C-N
1245(s)	1248(m)	δ (C-H) imi ring ipb
1159(w)	1164(m)	δ (C-H) 4HB- ring ipb
1118(w)	1144(m)	ν C-N
1052(w)	1046(w)	δ (C-H) 4HB- ring ipb
873(w)		δ (C-H) 4HB- ring opb
847(w)	855(s)	δ (C-C) imi ring
781(w)		$\delta\rho$ COO ⁻
749(w)	754(w)	δ (C-H) opb
692(w)		δ (C-H) opb
628(s)	633(m)	δ_s (COO ⁻)
535(s)		δ (C-N)
501(w)		δ (C-N)
437(w)		$\delta\omega$ (COO ⁻)

observed within the spectral range of 4000 to 400 cm⁻¹. Furthermore, the presence of N-H \cdots O and O-H \cdots O hydrogen bonding significantly influences the shifts in the positions of deformational modes of vibrations and has an impact on their intensity.

The X-ray crystal structure of I4HB clearly validates the protonation of the endocyclic nitrogen (N2) atom in imidazole, establishing intermolecular interactions with the oxygen (O1 and O2) atoms of

the carboxylate group within the 4-hydroxybenzoate anion. Vibrational peaks associated with NH₃⁺, C-N, and C-H stretching modes predominantly manifest in the high wavenumber region (3500-1500 cm⁻¹)²⁷. These N-H stretching wavenumbers experience a redshift due to the influence of intermolecular interactions, while their deformation modes undergo a blue shifted²⁸. Typically, N-H \cdots O intermolecular interactions are predicted to result in a broad peak within the infrared spectrum's range between 2100 and 1870 cm⁻¹. In the FTIR spectrum of the I4HB compound, a broad peak is indeed observed at 2034 cm⁻¹, indicating the presence of N-H \cdots O intermolecular interactions. Protonated NH⁺ species typically manifest in the spectral region between 3300 and 2500 cm⁻¹.

A weak intensity peak at 3385 cm⁻¹ corresponds to the N-H \cdots O stretching vibration. Similarly, the vibrational modes associated with O-H \cdots O intermolecular interactions are discerned with weak intensity at 3155 cm⁻¹ (FTIR) and 3174 cm⁻¹ (FT-Raman). A strong intensity peak at 3068 cm⁻¹ in the FT-Raman spectrum corresponds to the aromatic C-H stretching vibration. The peaks appearing at 1615 cm⁻¹ (FTIR) and 1604 cm⁻¹ (FT-Raman), both with strong intensity, arise from the asymmetric stretching vibration of the carboxylate (COO⁻) group present in the 4HB- anion. The symmetric stretching vibration is detected at 1430 cm⁻¹ (w) in FTIR and 1425 cm⁻¹ (m) in FT-Raman spectra. The aromatic C-C ring stretching of the 4HB- anion is observed at 1538 cm⁻¹ (w) in FTIR and 1530 cm⁻¹ (m) in FT-Raman spectra. A strong intensity peak at 1364 cm⁻¹ in both spectra is assigned to the vibration of the C-N stretching mode present in the imidazolium cation. In the FTIR spectrum, the aromatic ring (C-H) in-plane bending vibrations are identified at 1159 cm⁻¹ (w) and 1052 cm⁻¹ (w) with corresponding vibrations appearing at 1164 cm⁻¹ (m) and 1046 cm⁻¹ (w) in the FT-Raman spectrum. Weak intensity peaks observed around 749 cm⁻¹ and 692 cm⁻¹ are attributed to the aromatic ring (C-H) out-of-plane bending vibrations. Additionally, the rocking, scissoring, and wagging vibrations of the carboxylate (COO⁻) group are noticed at 781 cm⁻¹ (w), 628 cm⁻¹ (s), and 437 cm⁻¹ (w) in the FTIR spectrum.

UV-Vis spectral analysis

The UV-Visible absorption analysis of I4HB reveals a lower cutoff wavelength at approximately 380 nm, as illustrated in Fig. 5. The grown I4HB crystal exhibits a

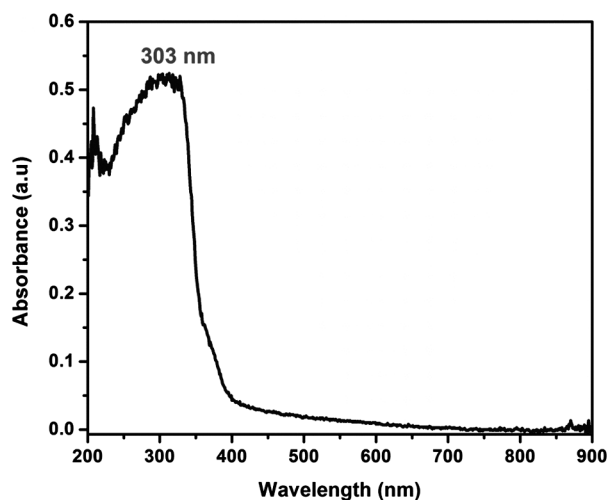


Fig. 5 — UV-visible absorption spectrum of I4HB

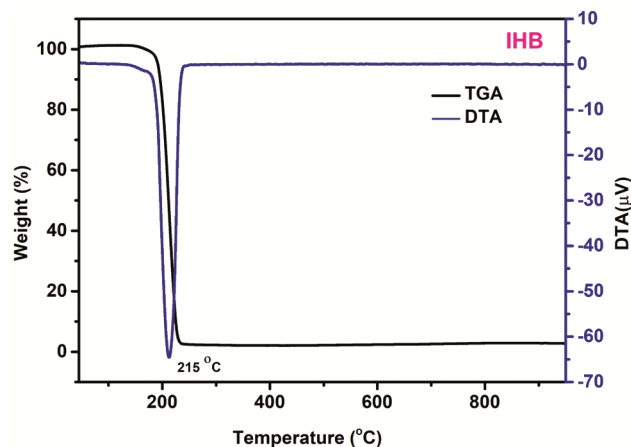


Fig. 6 — TG-DTA thermo curves of I4HB compound

wide transparency range in the visible spectrum, making it well-suited for optoelectronic applications. The optical absorption spectra indicate an absorption peak at 303 nm, attributed to the $n \rightarrow \pi^*$ transition. This broad transparency in both the visible and near-infrared regions suggests that the grown crystal holds significant potential for use in optoelectronic applications²⁹.

TG/DTA thermal analysis

Thermo Gravimetric – Differential Thermal Analysis (TG/DTA) was used to determine the thermal stability and melting point of I4HB, and the resulting thermal curve is shown in Fig. 6. The TG/DTA thermal study was carried out in a nitrogen environment at temperatures ranging from 30°C to 950°C at a heating rate of 10°C/min. No weight loss was recorded at 100°C during the thermal analysis of the formed crystal, confirming the lack of water molecules across the crystal lattice. In the TG curve, a

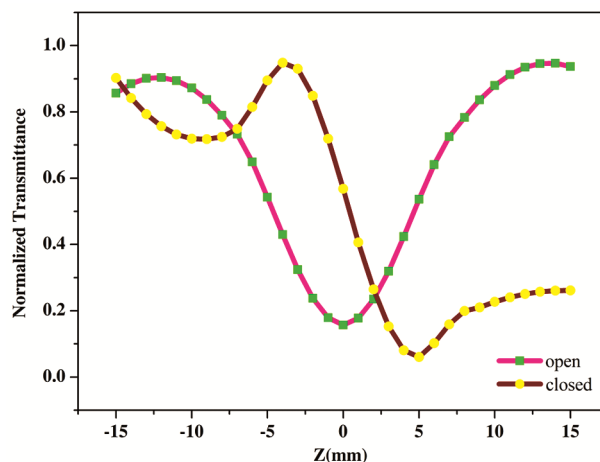


Fig. 7 — The normalized transmittance T when using the Self-focusing (open aperture) mode and the normalized transmittance T using the closed aperture mode in the distant field of I4HB crystal as an outcome of length Z along the lens axis.

weight loss of 96.3% was recorded at 214°C. Meanwhile, the DTA curve exhibited a distinct endothermic peak at 215°C, attributed to the decomposition of volatile substances such as CO_2 , CO , N , CH_2 molecules, and imidazole fragments. Based on the TG/DTA analysis results, it can be inferred that I4HB crystals demonstrate remarkable thermal stability, enduring temperatures of up to 215°C and can be effectively employed in optoelectronic device applications.

Z-Scan measurements

The Z-scan technique has gained significant recognition within the nonlinear optics community, serving as a standard method for accurately measuring intensity-dependent non-linear susceptibility, nonlinear refractive value (n_2), and the coefficient of nonlinear absorption (β)³⁰. In Fig. 7, the open aperture curve for I4HB is illustrated. It is noteworthy that a typical Z-scan result with a completely open aperture demonstrates insensitivity in nonlinear refraction. This method has become widely accepted due to its precision and reliability in characterizing nonlinear optical properties. It also shows the closed aperture arrangement for I4HB. In transmittance, the pattern comprises a peak followed by a trough, indicating negative nonlinearity. The self-defocusing effect occurs as a result of local fluctuations in refractive index rising intensity. As a result, the findings are predicted to be symmetric with regard to the focus.

A minimal transmittance is exhibited at the focus (valley) in materials with multi-photon absorption,

whereas a maximum transmittance is recorded at the focus (peak) in saturable absorber crystals. Multi-photon absorption reduces the peak while increasing the valley, whereas saturation does the reverse. The nonlinear refractive index (n_2), nonlinear absorption coefficient, and third-order susceptibility of I4HB are calculated to be $-8.87228 \times 10^{-9} \text{ cm}^2/\text{W}$, $3.39139 \times 10^{-5} \text{ cm/W}$, and $2.6623 \times 10^{-8} \text{ esu}$, respectively. The existence of self-defocusing nonlinearity is shown by the minus sign associated with the nonlinear refractive index, underlining the title compound's potential as a nonlinear optical (NLO) material³¹.

Conclusion

The organic single crystal imidazolium 4-hydroxybenzoate (I4HB) was generated at ambient temperature adopting the solvent slow evaporation process with ethanol as the solvent. I4HB has monoclinic symmetry corresponding to the $P2_1/n$ space group, according to X-ray diffraction (XRD) research. Various analytical methods, particularly ^1H and ^{13}C NMR, Fourier-transform infrared (FTIR), and FT-Raman spectroscopy, were used to confirm the molecular structure of I4HB. The UV-visible spectrum demonstrated that the I4HB crystal has a lower cut-off wavelength of 380 nm. Thermal analysis using TG/DTA indicated that I4HB remains thermally stable up to a temperature of 215°C. A Z-scan investigation was also performed to establish the third-order nonlinear property of I4HB, indicating its intrinsic self-defocusing properties for nonlinear optical applications.

CRedit authorship contribution statement

E. Shobhana: Conceptualization, Methodology, Data curation, Formal analysis, Validation, Writing – original draft, Writing – review and editing. B. Babu: Writing – original draft, Writing – review and editing. R. Kannan: Writing – original draft, Writing – review and editing. R. Thirumurugan: Software validation, Writing – review and editing. All the authors read and approved the final version of the manuscript.

Declaration of competing interest

The authors declare that they have no known competing financial interests or personal relationships that could have appeared to influence the work reported in this paper.

References

- McNamara D P, Childs S L, Giordano J, Iarriccio A, Cassidy J, Shet M S, Mannion R, O'Donnell E, & Park A, *Pharm Res*, 23 (2006) 1888.
- Blagden N, Matas M, Gavan P T & York P, *Adv. Drug Deliv Rev*, 59 (2007) 617.
- Samie A, Desiraju G R & Banik M, *Cryst Growth Des*, 17 (2017) 2406.
- Lemmerer A, Bernstein J & Kahlenberg V, *Cryst Eng Comm*, 12 (2010) 2856.
- Sasikala V, Sajan D, Sabu K J, Arumanayagam T & Murugakoothan P, *Spectrochim Acta A Mol Biomol Spectrosc*, 139 (2015) 555.
- Amalanathan M, Joe I H & Rastogi V K, *Spectrochim Acta A Mol Biomol Spectrosc*, 108 (2013) 256.
- Manimaran D, John C J, Rastogi V K & Joe I H, *Spectrochim Acta A Mol Biomol Spectrosc*, 109 (2013) 173.
- Shobhana E, Kesavasamy R, Babu B & Karunathan R, *Dig J Nanomat Biostr*, 17 (2022) 369.
- Vivek P & Murugakoothan P, *Opt Laser Tech*, 49 (2013) 288.
- Thirumurugan R & Anitha K, *J Mol Struct*, 1155 (2018) 267.
- Ji C, Chen T, Sun Z, Ge Y, Lin W, Luo J, Shi Q & Hong M, *Cryst Eng Comm*, 15 (2013) 2157.
- Aitipamula S, Wong A B, Chow P S & Tan R B, *Cryst Eng Comm*, 15 (2013) 5877.
- Vangala V R, Chow P S & Tan R B, *Cryst Eng Comm*, 3 (2011) 759.
- Mukherjee A, Tothadi S, Chakraborty S, Ganguly S & Desiraju G R, *Cryst Eng Comm*, 15 (2013) 4640.
- Childs S L, Stahly G P & Park A, *Mol Pharm*, 4 (2007) 323.
- Aitipamula S, Chow P S & Reginald B H Tan, *Cryst Eng Comm*, 14 (2012) 2381.
- Ghosh S, Bag P P & Reddy C M, *Cryst Growth & Des*, 11 (2011) 3489.
- Chinnakannu E, Sankar M, Chandran S, Thamotharan K & Manickam S, *J Mater. Sci: Mater. Electron*, 34 (2023) 1187.
- Ghosh K, Datta M, Fröhlich R & Ganguly N C, *J Mol Struct*, 737 (2005) 201.
- Zhao P S, Wang X, Jian F F, Zhang J L & Xiao L H, *J Serbian Chem Soc*, 75 (2010) 459.
- Sheldrick G M, 1997, SHELXS97 Program for Crystal Structure Solution, University of Göttingen, Germany. Program for crystal structure refinement. University of Göttingen, Germany.
- Farrugia L J, *J Appl Crystal*, 45 (2012) 849.
- Macrae C F, Bruno I J, Chisholm J A, Edgington P R, McCabe P, Pidcock E, Rodriguez-Monge L, Taylor R, Streek J V D & Wood P A, *J Appl Crystallogr*, 41 (2008) 466.
- Fuller J, Carlin R T, Simpson L J & Furtak T E, *Chem Mater*, 7 (1995) 909.
- Trivedi D R, Ballabh A & Dastidar P, *Cryst Eng Comm*, 5 (2003) 358.
- Bernstein J, Davis R E, Shimoni & Chang N L, *Angew Chem Int Ed Engl*, 34 (1995) 1555.
- Krishnakumar V, Nagalakshmi R & Janaki P, *Spectrochim Acta A Mol Biomol Spectrosc*, 61 (2005) 1097.
- Socrates G, *Infrared and Raman Characteristic Group Frequencies*, 3rd Ed, (John Wiley & Sons Ltd, England). 2001
- Shobhana E, Kesavasamy R, Arul H, Thirumurugan R & Babu B, *J Mol Struct*, 1204 (2020) 127516.
- Thirumurugan R Anitha, K, *Mater Lett*, 206 (2017) 30.
- Mostaghni F, *Acta Chim Slov*, 68 (2021) 170.